

LETTER

Open Access



Heterogeneous mantle anisotropy and fluid upwelling: implication for generation of the 1891 Nobi earthquake

Takashi Iidaka^{1*}, Yoshihiro Hiramatsu² and The Research Group for the Joint Seismic Observations at the Nobi Area

Abstract

The 1891 Nobi earthquake was the largest historic intraplate earthquake in Japan. The rupture origin corresponds to a zone of high strain rate inferred from geodetic data. To understand the geologic setting of this event, we deployed temporary seismic stations in the area. Shear-wave splitting analysis was performed using data from temporary and permanent seismic stations, revealing significant lateral variations in polarization directions. Polarization directions of NE–SW, ESE–WNW, and ENE–WSW were observed in the northeastern, central, and southwestern parts of the study area, respectively. The NE–SW- and ENE–WSW-aligned polarizations are consistent with the subduction directions of the Philippine Sea plate and Pacific plate, respectively; thus, shear-wave splitting in the northeastern and southwestern regions of the study area is likely caused by mantle wedge anisotropy, a consequence of mantle flow caused by the subducting oceanic slabs. However, the ESE–WNW orientations observed in the central Chubu Region are inconsistent with the subduction direction of either slab. Regions of low seismic velocity and low resistivity have been reported in the inferred position of the mantle wedge; these heterogeneities are thought to be caused by fluid rising from the dehydrated oceanic slabs. Thus, the ESE–WNW polarization in central Chubu could be a consequence of structural heterogeneities created by fluid to the crust from the mantle. The presence of crustal fluid is closely related to weakening, and the faults responsible for the 1891 Nobi earthquake are located just above the anisotropic region. Because fluids in the crust weaken the surrounding rock, this could explain the occurrence of the 1891 Nobi earthquake.

Keywords: Shear-wave splitting, Anisotropy, Nobi earthquake, Fault

Introduction

It is well known that elastic anisotropy in the Earth's mantle is closely related to mantle dynamics. Sources of seismic anisotropy in the crust and mantle have been extensively investigated. Two widely accepted models of such anisotropy are olivine crystal alignment in the upper mantle (Hess 1964; Francis 1969; Fuchs 1977; Ando et al. 1983) and fracture alignment in the shallow crust (Nur and Simmons 1969; Gupta 1973; Crampin 1978; Crampin et al. 1980). The most widely supported model of mantle

anisotropy is olivine alignment. The most common mantle constituent is olivine, and olivine crystals are thought to align in the direction of mantle flow, thereby generating anisotropy via the preferred orientations of the crystals. Shear-wave splitting analysis is one of the most commonly used tools to detect anisotropy and infer mantle flow direction (e.g., Silver and Chan 1991). Beneath Japan, the Pacific and Philippine Sea plates are subducting beneath the Eurasian plate to the west and northwest, respectively. Complex mantle flow with different flow directions is therefore expected, and the flow directions can be estimated from observed directions of mantle anisotropy polarization.

Fracture alignment is widely invoked to explain observations of seismic anisotropy in the crust (e.g., Kaneshima

*Correspondence: iidaka@eri.u-tokyo.ac.jp

¹ Earthquake Research Institute, University of Tokyo, Yayoi 1-1-1, Bunkyo, Tokyo, Japan

Full list of author information is available at the end of the article

1990). In this model, shear-wave splitting in the crust is caused by the orientations of faults or cracks, and it is thought that propagating cracks are preferentially aligned subparallel to the orientation of the axis of maximum stress. This, in turn, means that the “fast” direction of shear waves should also be oriented subparallel to the axis of maximum stress (Crampin 1978). Heterogeneous structures in the upper mantle can generate anisotropy by a similar fracture alignment process (e.g., Iidaka and Obara 1995). Iidaka and Obara (1995) detected anisotropic regions in the mantle wedge beneath central Japan. The anisotropic regions correspond to zones of low seismic velocity and low Q ; this region is therefore thought to result from heterogeneous structures formed by fluid rising from the mantle wedge.

Data from a high-density Global Navigation Satellite System (GNSS) array study, operated by the Geospatial Information Authority of Japan (GSI), indicate a zone of high strain rate along the Japan Sea coastline (e.g., Sagiya et al. 2000). This zone has been termed the Niigata–Kobe Tectonic Zone (NKTZ). Many large historic earthquakes have occurred in the NKTZ, including the magnitude 8 Nobi earthquake of October 28, 1891. This event is Japan’s strongest known intraplate earthquake. The maximum size of typical intraplate earthquakes in Japan is ~ 7 ; however, during the Nobi earthquake the rupture propagated along three different faults: the Nukumi, Neodani, and Umehara faults.

The faults of the 1891 Nobi earthquake are all located in the NKTZ. Intraplate earthquakes occur as a result of stress concentration and strain accumulation on crustal faults. Understanding the tectonic setting of large intraplate earthquakes is important in earthquake hazard mitigation. Recently, it has been suggested that the presence of crustal fluid is closely related to the triggering of intraplate earthquakes. Iio et al. (2002) proposed a model that explains the cause of some intraplate earthquakes, whereby a weak zone in the lower crust deforms relatively easily, resulting in a high concentration of stress above it.

Many previous studies have investigated how the presence of fluid in the lower crust affects intraplate earthquakes (Eberhart-Phillips and Michael 1993; Johnson and McEvilly 1995; Zhao et al. 1996; Hasegawa et al. 2009). Fluid released from the upper mantle and lower crust is closely related to the mechanical state of the crust, as fluid plays an important role in crustal weakening. Zones of low resistivity are generally located in the deeper part of an active fault (e.g., Ogawa et al. 2001; Becken and Ritter 2012), and conductivity in the crust is sensitive to interconnected fluids in rock. Fluids under high pressures reduce the strain thresholds of rocks and facilitate brittle failure within the upper crust (e.g., Byerlee 1990).

Thus, fluids in interconnected porosity networks can strongly influence deformation along fault zones.

The Research Group for the Joint Seismic Observations at the Nobi Area deployed 43 temporary seismic stations in an 80×80 km area, including the source faults of the 1891 Nobi earthquake, to better understand the tectonic setting of such a large intraplate event. Shear-wave splitting was investigated using both temporary and permanent seismic stations.

Data

The data used in this experiment were recorded by temporary seismic stations deployed by the Research Group for the Joint Seismic Observations at the Nobi Area and permanent Hi-net stations operated by the National Research Institute for Earth Science and Disaster Prevention (NIED; Okada et al. 2004). A station map is shown in Fig. 1. Most seismic stations had three-component sensors with a natural frequency of 1 Hz.

Our data set consisted of earthquakes located deeper than 230 km that occurred between January 1, 2009, and December 31, 2014 (Fig. 1; Table 1). Only seismic rays with incidence angles of $<30^\circ$ were used, to avoid waveform distortion due to the phase shift between the SH and SV components (e.g., Nuttli 1961; Mendiguren 1969), as the use of such waves could lead to false detections of shear-wave anisotropy.

Methods

Shear-wave splitting is usually expressed in terms of two parameters: fast polarization azimuth, ϕ (in degrees), and time lag, τ (in seconds), which is the delay between the fast and slow arrivals. We investigate shear-wave splitting using techniques based on Fukao (1984). A band-pass filter with a frequency window of 0.5–8 Hz is applied to all waveform data. We pick S waves manually from individual seismograms. We then calculate the cross-correlations of the two horizontal components of motion over the ranges $\phi = -90^\circ$ to $+90^\circ$ and a window of 4 s, in increments of 1° and 0.01 s, respectively. We choose the time lag τ and fast polarization azimuth ϕ that yield the maximum correlation (Fig. 2). To confirm the resultant splitting parameters, we calculate anisotropy-corrected seismograms. The anisotropy-corrected particle motion is linear (Fig. 2d), as expected for a double-couple source mechanism. Low-quality waveform data with poor signal-to-noise ratios (SNR) are removed using the data with maximum cross-correlation coefficients of >0.75 . The linear polarizations obtained from anisotropy-corrected data suggest that observed waveform splitting is caused by an anisotropic medium, rather than seismic noise.

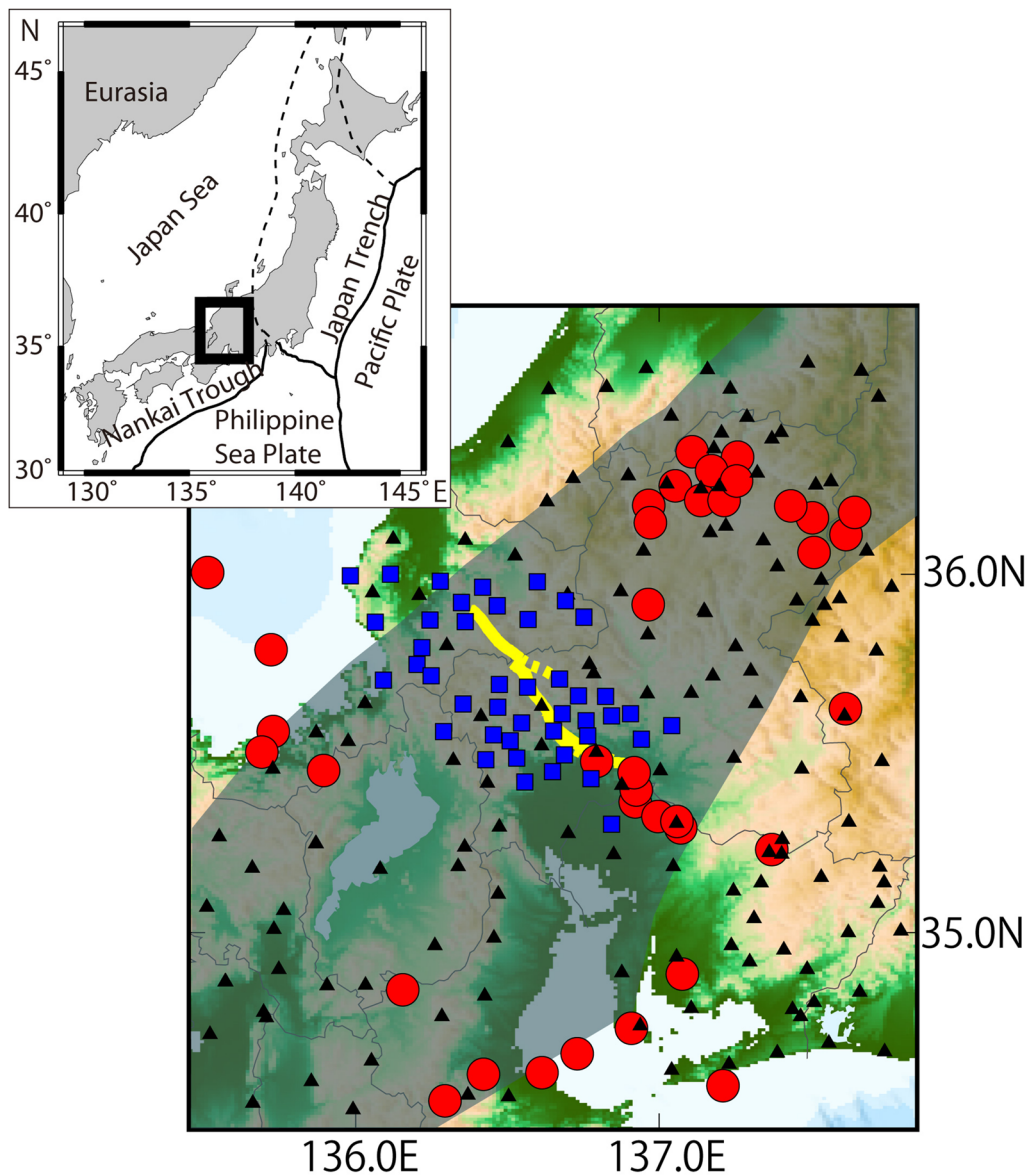


Fig. 1 Location map of seismic stations and earthquakes. *Red circles* denote epicenters of deep earthquakes. *Black triangles* indicate permanent seismic stations operated by Hi-net and universities. *Blue squares* indicate temporary seismic stations operated during this study. The *lightly shaded area* denotes the NKTZ. *Yellow lines* are faults that ruptured during the 1891 Nobi earthquake. The location of the research area (*black square*) is shown in the *inset*

Results and discussion

Heterogeneous mantle anisotropy and its origin

Based on spatially distinct groups of earthquake hypocenters, the research area is divided into four regions denoted as a–d in Fig. 3. Shear-wave splitting data in each subfigure were obtained from earthquakes in the plotted region.

Region A is located in the northeastern part of the study area (Fig. 3a). The depths of the earthquakes are 230–290 km. The polarization direction data show

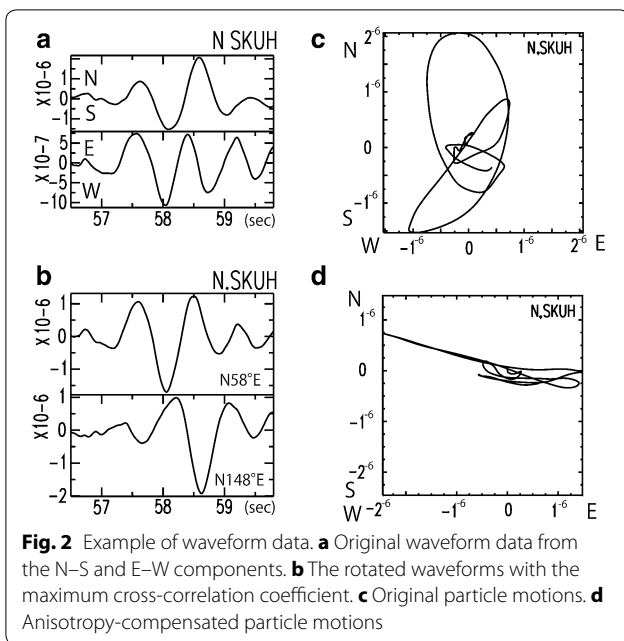
significant lateral variations: Polarization directions align NE–SW in the northern part of the region and ESE–WNW in the southern part. The polarization directions from region B also show lateral variations: Using earthquakes with depths of 250–320 km, the polarization directions align ESE–WNW in the southern part of the region, with a maximum time delay of ~2 s (Fig. 3b). Notably, the faults ruptured by the 1891 Nobi earthquake are located in this area. Results for region C, in the southern part of the research area, are shown in Fig. 3c. Here,

Table 1 List of earthquakes

Origin time									
Yr	Mo	Day	Hr	Min	Sec	Long (°)	Lat (°)	Dep. (km)	M
2009	03	03	09	15	48.43	137.0533	36.2465	267.63	3.6
2009	03	12	22	50	49.92	137.2590	36.3262	268.16	3.6
2009	06	10	13	07	2.96	136.6148	34.6083	354.58	5.0
2009	08	07	14	04	40.10	137.1373	36.2055	270.76	3.6
2009	12	11	19	32	52.36	137.6165	36.1100	236.76	3.9
2010	01	12	03	01	5.67	136.7955	35.4787	307.78	3.7
2010	01	20	23	44	51.23	137.0710	35.2917	319.46	3.6
2010	03	01	09	08	50.19	136.9218	35.3648	308.53	3.5
2010	03	09	02	08	12.75	137.5067	36.1567	238.21	3.9
2010	07	06	00	48	36.02	135.7212	35.7890	346.18	4.7
2010	08	27	00	08	4.23	136.9672	36.1918	285.77	5.2
2011	02	24	06	17	9.24	136.9655	35.9147	276.22	3.7
2011	03	25	07	07	17.12	137.6143	35.6253	250.75	4.0
2011	04	30	13	30	24.50	135.7293	35.5617	349.94	3.6
2011	09	10	23	55	45.58	135.8947	35.4525	343.01	3.5
2011	10	30	01	50	41.34	137.2112	34.5730	328.76	3.8
2012	01	11	12	54	34.10	136.9963	35.3238	300.27	3.9
2012	01	22	07	07	20.35	137.6452	36.1722	233.02	3.7
2012	01	30	02	01	45.70	136.9090	34.7333	341.14	4.5
2012	03	15	03	58	17.58	136.7302	34.6620	347.34	4.1
2012	04	27	18	26	55.39	136.4215	34.6035	359.04	3.7
2012	07	09	09	34	8.44	137.5112	36.0608	258.20	3.6
2012	08	05	03	28	55.67	137.4345	36.1900	256.97	3.8
2012	10	13	12	08	58.64	136.9255	35.3977	300.84	3.5
2013	01	15	01	20	5.33	137.2152	36.2058	267.19	3.7
2013	04	04	23	20	23.65	136.9727	36.1433	272.92	3.9
2013	08	22	00	34	49.32	137.0600	35.3103	300.58	3.5
2013	10	31	12	02	33.74	137.1088	36.3413	273.86	3.5
2013	11	03	23	52	3.28	137.1743	36.2892	258.34	3.6
2013	11	05	12	40	55.45	136.1550	34.8402	349.61	4.0
2014	01	24	10	43	51.54	137.2550	36.2597	261.72	4.2
2014	02	19	16	57	0.07	137.0770	34.8833	346.54	3.5
2014	10	07	06	42	44.01	136.9187	35.4465	311.32	3.5
2014	10	24	22	30	53.71	137.3715	35.2322	278.74	3.8
2014	11	27	01	55	14.28	135.5133	36.0047	351.98	3.7
2014	12	04	04	10	48.68	136.2957	34.5303	366.49	3.5
2014	12	06	01	01	56.79	135.6912	35.5040	351.78	4.8

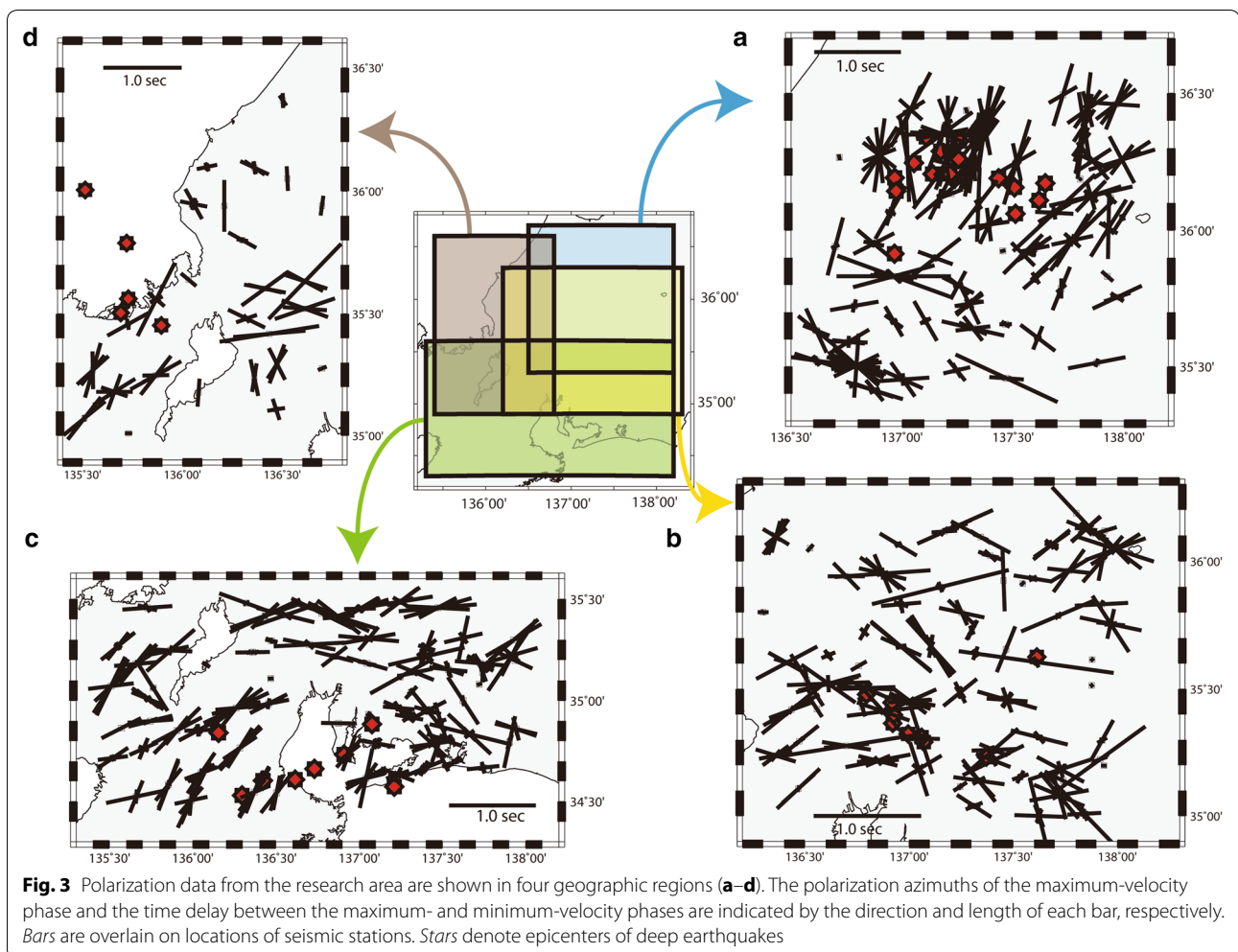
the depths of the earthquakes used are 320–370 km, and the most common polarization direction is ENE–WSW. Polarization data from region D again suggest large lateral variations (Fig. 3d). Using earthquakes with focal depths of 340–355 km, we find that polarizations from the central part of region D align ENE–WSW, consistent with region C; yet, in the southeastern and northeastern parts of the region, polarizations align N–S and delay times are small.

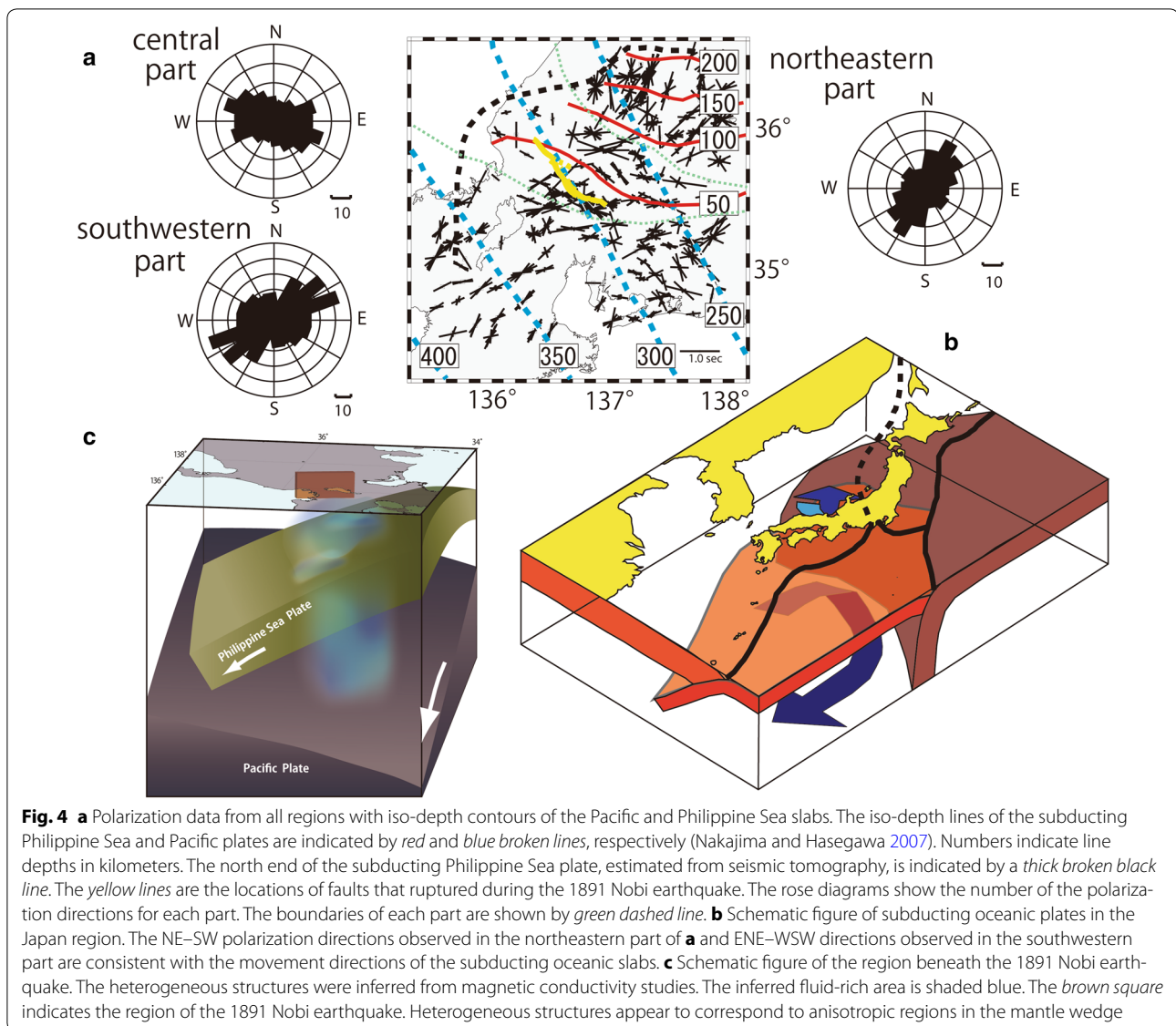
The entirety of the polarization data set (obtained from all four regions) is plotted in Fig. 4a. Large lateral variations are clearly visible, and some remarkable characteristics can be seen. The polarizations are aligned NE–SW in the northeastern part of the study area, ESE–WNW in the central part, and ENE–WSW in the southwestern part (Fig. 4a). Near the boundaries of each polarization group, the directions are less uniform. At the border area of the polarization groups, the rays propagate both of the



anisotropic regions. We suppose that the data are scattered and less uniform. We now discuss the potential causes of anisotropy in each area. The earthquakes used here are all deep earthquakes in the subducting Pacific plate, with focal depths of 230–370 km. Their ray paths thus propagate through the mantle wedge and crust; we must therefore consider both crustal and mantle anisotropy as possible sources of the observed anisotropy.

Most of the observed time delay values are larger than 0.5 s. Crustal anisotropy in Japan has been described in many studies (e.g., Kaneshima 1990; Hiramatsu et al. 2015). It has been suggested that the maximum possible time delay of shear-wave splitting due to crustal anisotropy is <0.2 s for Japan (Kaneshima 1990). Hiramatsu et al. (2015) studied crustal anisotropy in the area of the 1891 Nobi earthquake using the same temporary seismic network as in this study and suggested that the maximum time delay in this area was <0.12 s. The observed time delays in this study are much larger than those values; we





therefore conclude that the observed splitting is caused mainly by mantle anisotropy.

We consider two possible causes for the observed anisotropy: olivine alignment (e.g., Silver and Chan 1991) and structural heterogeneities (e.g., Iidaka and Obara 1995). Iso-depth lines of the Philippine Sea and Pacific plates are shown in Fig. 4a, adapted from Nakajima and Hasegawa (2007) and Zhao and Hasegawa (1993), respectively. NE–SW polarization, which dominates in the northeastern part of the research area, is highly consistent with the subduction direction of the Philippine Sea slab. Anisotropy in this region had been studied by many researchers (e.g., Ando et al. 1983; Iidaka et al. 2009; Hiramatsu et al. 1998). In this area, the geometry of the subducting Philippine Sea plate has been extensively

studied (e.g., Nakajima and Hasegawa 2007): It is widely accepted that the dip direction of the Philippine Sea slab in this region is northeast. The plate motion direction of the Philippine Sea plate has been studied by many scientists (e.g., Demets et al. 2010). The direction of the Philippine Sea plate was estimated to NW at the Nankai Trough. But, the driving force of the plate is considered as the negative buoyancy of the cold slab (e.g., Forsyth and Uyeda 1975). The mantle flow is caused by the subducting slab. The direction of the mantle flow should be parallel to the subduction direction.

The causes of anisotropy in mantle are well studied (e.g., Hess 1964; Francis 1969; Fuchs 1977) and usually interpreted as a result of olivine crystal alignment. Olivine is a major mantle constituent, and it becomes

anisotropic with only modest amounts of crystal alignment; crystals align in the direction of mantle flow, and the resultant polarization direction is parallel to the flow direction.

The preferred orientation of the olivine crystal is expected to be parallel to the plate subduction. Thus, the observed NE–SW polarizations are consistent with the subduction direction of the Philippine Sea slab (Fig. 4a). We can therefore assume that the direction of mantle flow corresponds to the direction of shear-wave splitting polarization; it follows that the NE–SW-aligned polarizations can be explained by mantle flow related to the subducting Philippine Sea slab. A high-density network of temporary seismometers was deployed in this area by The Japanese University Group of the Joint Seismic Observations at NKTZ (2005). Iidaka et al. (2009) studied shear-wave splitting in the region and found clear fine-scale lateral variations in polarization directions, consistent with the subduction direction of the Philippine Sea slab. Thus, our findings are consistent with the results of Iidaka et al. (2009).

Next, we discuss the possible source of the ENE–WSW polarizations observed in the southwestern part of the research area (Fig. 3c). Hiramatsu et al. (1998) studied seismic anisotropy in central Japan, including the southern part of the target area of the present study, and estimated depth variations in anisotropy using a dense set of ray paths. The anisotropic region found in their study was consistent with a low-velocity region obtained from seismic tomography (Hirahara et al. 1989; Sekiguchi 1991); thus, they concluded that the cause of the anisotropy was related to the heterogeneous structures created by fluid-filled cracks. Nakamura et al. (2008) found velocity perturbations that suggested a low- V_p region at depths of ~100–150 km beneath the eastern part of our study area; however, there was no corresponding low- V_s region at the same depths. If the cause of the anisotropy is truly fluid-filled cracks, then the area should be characterized by low- V_s and low- Q regions (e.g., Iidaka and Obara 1995; Hiramatsu et al. 1998). It follows that the anisotropy found in the present study is unlikely to result from structural heterogeneities associated with fluid-filled cracks. Instead, the well-resolved direction of subduction of the Pacific plate (e.g., Zhao and Hasegawa 1993) is consistent with the alignment of the observed polarizations. We therefore suggest that the anisotropy in these regions could be caused by the alignment of olivine crystals in the mantle wedge. The crystal alignment is expected to result from mantle flow related to subduction of the Pacific plate.

The NE–SW and ENE–WSW orientations can be explained by anisotropy caused by olivine alignment related to the subducting oceanic slabs (Fig. 4b).

However, this does not adequately explain the observed ESE–WNW polarizations in the central part of the research area (Fig. 4a). Beneath this area, two oceanic plates are descending with different directions. The Pacific plate is descending to WSW. The dip direction of the Philippine Sea slab is NE. The effects caused by the subducting two slabs have to be considered. However, the depth of the Philippine Sea slab is almost similar to that of the Moho boundary beneath the faults of Nobi earthquake (Nakajima et al. 2015). The thickness of the mantle wedge between the continental Moho and top of the Philippine Sea slab seems to be about 5–10 km at the area. The contribution to the shear-wave splitting caused by the flow related to Philippine Sea slab seems to be small.

Instead, we must consider other possible causes. Other explanations of the anisotropy in this area have been proposed by, for example, Iidaka and Obara (1995) and Hiramatsu et al. (1998). Iidaka and Obara (1995) studied seismic anisotropy in the mantle wedge in central Japan and found remarkable lateral variations: The magnitudes of shear-wave splitting time delays differed between the fore-arc and back-arc sides of the volcanic front, and the anisotropic region observed at the back-arc side of the volcanic front was characterized by low seismic velocity and low Q . Their interpretation was that the anisotropic region was caused by heterogeneous structure generated by fluid rising from the mantle wedge.

Relationship between fluids from the mantle and the generation of the 1891 Nobi earthquake

The area of ESE–WNW-aligned polarizations in Fig. 4a includes the faults that ruptured during the 1891 Nobi earthquake. Investigations of seismic velocity structure in the area have revealed the faults responsible for the earthquake. The relationship between crustal fluids and earthquakes has been studied previously, including studies of the controls of such fluids on intraplate earthquakes. A close relationship between the earthquake's fault zone and a subsurface low-velocity zone has been established (Eberhart-Phillips and Michael 1993; Johnson and McEvilly 1995; Zhao et al. 1996). A review of intraplate earthquakes in Japan found clear imaging of low-velocity zones and/or high- V_p/V_s zones near the rupture sources of many major earthquakes (Hasegawa et al. 2009), presumably related to the presence of lower crustal fluid; however, velocity structure alone is not sufficient to infer the presence of fluids. Geomagnetic surveys have found regions of low resistivity near many active faults, which could relate to the presence of fluids in the source area (Gupta et al. 1996; Tank et al. 2005; Wannamaker et al. 2009; Becken et al. 2011; Becken and Ritter 2012). In Japan, some close relationships between low-resistivity regions and earthquake faults have been proposed

(Mitsuhata et al. 2001; Yamaguchi et al. 2001; Uyeshima et al. 2005; Yoshimura et al. 2008). The characteristics of the relationships between faults and resistivity structures are summarized by Ogawa et al. (2001) and Becken and Ritter (2012). Low-resistivity zones are generally located in the deeper parts of active faults and are thought to be caused by fluids. Fluids released from the upper mantle are closely related to the mechanical state of the crust.

In the source region of the 1891 Nobi earthquake, seismic tomography reveals fine-scale P- and S-wave velocity structures in the crust and uppermost mantle underlying the faults of the earthquake (Nakajima et al. 2015). The lower crust beneath the Nukumi fault, corresponding to the northern extent of the Nobi earthquake rupture, contains a low-velocity zone. On the other hand, inferred seismic velocities beneath the Ume-hara fault, at the southern terminus of the rupture, are only moderate. In the uppermost mantle beneath the Nobi earthquake regions have seismic velocities ~15 % lower than the velocities expected for mantle peridotites. Across-fault variations in seismic velocity include a body of low P-wave velocity in the lower crust, partly underlying the southwestern region of the Nukumi fault. These results suggest fluids with volume fractions of 2–3 % are present in the local area, extending from the uppermost mantle to the middle crust beneath the Nukumi fault.

Resistivity is highly sensitive to the amount of crustal fluid present. The existence of a region of low resistivity near an active fault can be interpreted as evidence of crustal fluid in the source area. Local resistivity structure suggests the presence of crustal fluid (Uyeshima et al. 2013), including a region of low resistivity beneath the Nobi earthquake fault system. In this region, the depth to the Philippine Sea slab is ~50 km and the Pacific slab is located at depths of ~300 km. The region of low resistivity extends from the lower crust to the mantle wedge just above the Pacific slab and includes the Philippine Sea slab. Figure 4c shows a conceptual model of this interpretation: Fluid is released from the subducting Pacific slab by dehydration reactions and rises buoyantly from the mantle wedge. Additional fluid is contributed by the Philippine Sea slab; the resultant aggregation of fluid is large enough to reach the upper crust.

In this model, heterogeneous structures caused by rising fluid create the anisotropic medium. We consider the anisotropic region to be a result of fluid in the mantle, generated by dehydration of the subducting oceanic slabs. Fluid plays an important role in crustal weakening, and crustal conductivity is sensitive to interconnected fluids in rocks. Fluids at high pressures have the ability to reduce the strain thresholds of rocks and facilitate brittle failure within the upper crust (e.g., Byerlee 1990), while

fluids in interconnected porosity networks reduce the shear moduli, which can strongly influence deformation in fault zones.

Conclusions

We used seismic data from permanent networks and a temporary deployment of three-component sensors to investigate anisotropy in the rupture area of the 1891 Nobi earthquake, the largest known intraplate earthquake in Japan. Large lateral variations in azimuthal directions of shear-wave splitting were detected. In the northeastern Chubu Region, polarization aligns NE–SW; this can be explained by mantle flow related to subduction of the Philippine Sea plate. Polarization directions in the southwestern part of the Chubu Region align ENE–WSW, consistent with mantle flow related to the subducting Pacific plate. In central Chubu, however, polarizations align ESE–WNW, inconsistent with the subduction of either oceanic slab. This area is located just beneath the fault zone of the 1891 Nobi earthquake and overlies a mantle wedge corresponding to low seismic velocity and low electric resistivity. Anisotropy here is best explained by mantle heterogeneities related to fluid upwelling from the subducting slabs. Because these fluids drive crustal weakening, this explanation is consistent with fluid-weakened lower crust as the cause of the Nobi earthquake.

Abbreviations

GNSS: Global Navigation Satellite System; GSI: Geospatial Information Authority of Japan; JMA: Japan Meteorological Agency; NIED: National Research Institute for Earth Science and Disaster Prevention; NKTZ: Niigata–Kobe Tectonic Zone.

Authors' contributions

TI led and designed the whole research and drafted the manuscript. YH, support the whole research and drafted the manuscript. The Research Group for the Joint Seismic Observations at the Nobi Area designed and had operated the seismic stations. All authors read and approved the final manuscript.

Author details

¹ Earthquake Research Institute, University of Tokyo, Yayoi 1-1-1, Bunkyo, Tokyo, Japan. ² School of Natural System, College of Science and Engineering, Kanazawa University, Kanazawa, Japan.

Acknowledgements

We thank NIED and the Japan Meteorological Agency (JMA) for the use of their waveform data. Some of the figures presented here were constructed using the GMT code (Wessel and Smith 1991). This study was supported by the Ministry of Education, Culture, Sports, Science and Technology (MEXT) of Japan, under its Earthquake and Volcano Hazards Observation and Research Program. This work was also supported by JSPS KAKENHI Grant Number JP26109002.

Competing interests

The authors declare that they have no competing interests.

Received: 11 August 2016 Accepted: 27 September 2016

Published online: 18 October 2016

References

- Ando M, Ishikawa Y, Yamazaki F (1983) Shear-wave polarization anisotropy in the upper mantle beneath Honshu. *Japan J Geophys Res* 88:5850–5864
- Becken M, Ritter O (2012) Magnetotelluric studies at the San Andreas fault zone: implications for the role of fluids. *Surv Geophys* 33:65–105
- Becken M, Ritter O, Bedrosian PA, Weckmann U (2011) Correlation between deep fluids, tremor and creep along the central San Andreas fault. *Nature* 480:87–90
- Byerlee J (1990) Friction, overpressure and fault normal compression. *Geophys Res Lett* 17:2109–2112
- Crampin S (1978) Seismic-wave propagation through a cracked solid: polarization as a possible dilatancy diagnostic. *Geophys J R Astron Soc* 53:467–496
- Crampin S, Evans R, Ucer B, Doyle M, Davis JP, Yegorkina GV, Miller A (1980) Observations of dilatancy-induced polarization anomalies and earthquake prediction. *Nature* 286:874–877
- DeMets C, Gordon RG, Argus DF (2010) Geologically current plate motions. *Geophys J Int* 181:1–80. doi:10.1111/j.1365-246X.2009.04491.x
- Eberhart-Phillips D, Michael AJ (1993) Three-dimensional velocity structure, seismicity, and fault structure in the Parkfield Region, central California. *J Geophys Res* 98:15737–15758
- Forsyth D, Uyeda S (1975) On the Relative Importance of the Driving Forces of Plate Motion. *Geophys J R Astron Soc* 43:163–200
- Francis TJG (1969) Generation of seismic anisotropy in the upper mantle along the mid-oceanic ridges. *Nature* 221:162–165
- Fuchs K (1977) Seismic anisotropy of the subcrustal lithosphere as evidence for dynamical processes in the upper mantle. *Geophys J R Astron Soc* 49:167–179
- Fukao Y (1984) Evidence from core-reflected shear waves anisotropy in the Earth's mantle. *Nature* 309:695–698
- Gupta IN (1973) Premonitory variations in S-wave velocity anisotropy before earthquakes in Nevada. *Science* 182:1129–1132
- Gupta HK, Sarma SVS, Harinarayana T, Virupakshi G (1996) Fluids below the hypocentral region of Latur Earthquake, India; geophysical indicators. *Geophys Res Lett* 23:1569–1572
- Hasegawa A, Nakajima J, Uchida N, Okada T, Zhao D, Matsuzawa T, Umino N (2009) Plate subduction, and generation of earthquakes and magmas in Japan as inferred from seismic observations: an overview. *Gondwana Res* 16:370–400
- Hess HH (1964) Seismic anisotropy of the uppermost mantle under oceans. *Nature* 203:629–631
- Hirahara K, Ikami A, Ishida M, Mikumo T (1989) Three-dimensional P-wave structure beneath central Japan: low velocity bodies in the wedge portion of the upper mantle above high-velocity subducting plates. *Tectonophysics* 163:63–73
- Hiramatsu Y, Ando M, Tsukuda T, Ooida T (1998) Three-dimensional image of the anisotropic bodies beneath central Honshu, Japan. *Geophys J Int* 135:801–816
- Hiramatsu Y, Iidaka T, The Research Group for the Joint Seismic Observations at the Nobi Area (2015) Stress state in the upper crust around the source region of the 1891 Nobi earthquake through shear wave polarization anisotropy. *Earth Planets Space*. doi:10.1186/s40623-015-0220-4
- Iidaka T, Obara K (1995) Shear-wave polarization anisotropy in the mantle wedge above the subducting Pacific plate. *Tectonophysics* 249:53–68
- Iidaka T, Hiramatsu Y, The Japanese University Group of the Joint Seismic Observations at NKTZ (2009) Shear-wave splitting analysis of the upper mantle at the Niigata–Kobe tectonic zone with the data of the joint seismic observations at NKTZ. *Earth Planets Space* 61:227–235
- Iio Y, Sagiya T, Kobayashi Y, Shiozaki I (2002) Water-weakened lower crust and its role in the concentrated deformation in the Japanese Islands. *Earth Planet Sci Lett* 203:245–253
- Johnson PA, McEvilly TV (1995) Parkfield seismicity; fluid-driven? *J Geophys Res* 100:12937–12950
- Kaneshima S (1990) Origin of crustal anisotropy: shear wave splitting studies in Japan. *J Geophys Res* 95:11121–11133
- Mendiguren JA (1969) Study of focal mechanism of deep earthquakes in Argentina using non linear particle motion of S waves. *Bull Seismol Soc Am* 59:1449–1473
- Mitsuhashi Y, Ogawa Y, Mishina M, Kono T, Yokokura T, Uchida T (2001) Electromagnetic heterogeneity of the seismogenic region of 1962 M6.5 Northern Miyagi Earthquake, northeastern Japan. *Geophys Res Lett* 28:4371–4374
- Nakajima J, Hasegawa A (2007) Subduction of the Philippine Sea plate beneath southwestern Japan: slab geometry and its relationship to arc magmatism. *J Geophys Res*. doi:10.1029/2006JB004770
- Nakajima J, Kato A, Iwasaki T, The Research Group for the Joint Seismic Observations at the Nobi Area (2015) The weakened lower crust beneath the Nobi fault system, Japan: implications for stress accumulation to the seismogenic zone. *Tectonophysics* 655:147–160
- Nakamura M, Yoshida Y, Zhao D, Takayama H, Obana K, Katao H, Kasahara J, Kanazawa T, Kodaira S, Sato T, Shiohara H, Shinohara M, Shimamura H, Takahashi N, Nakanishi A, Hino R, Murai Y, Mochizuki K (2008) Three-dimensional P- and S-wave velocity structures beneath Japan. *Phys Earth Planet Inter* 168:49–70
- Nur A, Simmons G (1969) Stress induced anisotropy in rocks: an experimental study. *J Geophys Res* 74:6667–6674
- Nuttli O (1961) The effect of the earth's surface on the S wave particle motion. *Bull Seismol Soc Am* 51:237–246
- Ogawa Y, Mishina M, Goto T, Satoh H, Oshiman N, Kasaya T, Takahashi Y, Nishitani T, Sakanaka S, Uyeshima M, Takahashi Y, Honkura Y, Matsushima M (2001) Magnetotelluric imaging of fluids in intraplate earthquake zones, NE Japan Back Arc. *Geophys Res Lett* 28:3741–3744
- Okada Y, Kasahara K, Hori S, Obara K, Sekiguchi S, Fujiwara H, Yamamoto A (2004) Recent progress of seismic observation networks in Japan—Hi-net, F-net, K-NET and KiK-net—. *Earth Planets Space* 56:xv–xxvii
- Sagiya T, Miyazaki S, Tada T (2000) Continuous GPS array and present-day crustal deformation of Japan. *Pure Appl Geophys* 157:2303–2322
- Sekiguchi S (1991) Three dimensional Q-structure beneath Kanto-Tokai district, Japan. *Tectonophysics* 195:83–104
- Silver PG, Chan WW (1991) Shear wave splitting and subcontinental mantle deformation. *J Geophys Res* 96:16429–16454
- Tank SB, Honkura Y, Ogawa Y, Matsushima M, Oshiman N, Tunçer MK, Çelik C, Tolak E, İşikara AM (2005) Magnetotelluric imaging of the fault rupture area of the 1999 İzmit (Turkey) earthquake. *Phys Earth Planet Int* 150:213–225
- The Japanese University Group of the Joint Seismic Observations at NKTZ (2005) The university joint seismic observations at the Niigata–Kobe Tectonic Zone. *Bull Earthq Res Inst Univ Tokyo* 80:133–147
- Uyeshima M, Ogawa Y, Honkura Y, Koyama S, Ujihara N, Mogi T, Yamaya Y, Harada M, Yamaguchi S, Shiozaki I, Noguchi T, Kuwaba Y, Tanaka Y, Mochido Y, Manabe N, Nishihara M, Saka M, Serizawa M (2005) Resistivity imaging across the source region of the 2004 Mid-Niigata Prefecture earthquake (M6.8), central Japan. *Earth Planets Space* 57:441–446
- Uyeshima M, Yamaguchi S, Murakami H, Tanbo T, Yoshimura R, Ichihara H, Omura K (2013) Electrical conductivity structure beneath backarc side of Chubu District, Central Japan, revealed by the Network-MT. Abstract of Japan Geoscience Union Meeting 2013 S5526-06
- Wannamaker PE, Caldwell TG, Jiracek GR, Maris V, Hill GJ, Ogawa Y, Bibby HM, Bennie SL, Heise W (2009) Fluid and deformation regime of an advancing subduction system at Marlborough, New Zealand. *Nature* 460:733–736
- Wessel P, Smith WHF (1991) Free software helps map and display data. *EOS Trans AGU* 72:441
- Yamaguchi S, Murakami T, Inokuchi H (2001) Resistivity mapping using the VLF-MT method around surface fault ruptures of the 1995 Hyogo-ken Nanbu earthquake, Japan. *Island Arc* 10:296–305
- Yoshimura R, Oshiman N, Uyeshima M, Ogawa Y, Mishina M, Toh H, Sakanaka S, Ichihara H, Shiozaki I, Ogawa T, Miura T, Koyama S, Fujita Y, Nishimura K, Takagi Y, Imai M, Honda R, Yabe S, Nagaoka N, Tada M, Mogi T (2008) Magnetotelluric observations around the focal region of the 2007 Noto Hanto Earthquake (Mj 6.9), Central Japan. *Earth Planets Space* 60:117–122
- Zhao D, Hasegawa A (1993) P wave tomographic imaging of the crust and upper mantle beneath the Japan Islands. *J Geophys Res* 98:4333–4353
- Zhao D, Kanamori H, Negishi H, Wiens DA (1996) Tomography of the source area of the 1995 Kobe earthquake; evidence for fluids at the hypocenter? *Science* 274:1891–1894